NJC

Accepted Manuscript

This is an *Accepted Manuscript*, which has been through the Royal Society of Chemistry peer review process and has been accepted for publication.

Accepted Manuscripts are published online shortly after acceptance, before technical editing, formatting and proof reading. Using this free service, authors can make their results available to the community, in citable form, before we publish the edited article. We will replace this *Accepted Manuscript* with the edited and formatted *Advance Article* as soon as it is available.

You can find more information about *Accepted Manuscripts* in the Information for Authors.

Please note that technical editing may introduce minor changes to the text and/or graphics, which may alter content. The journal's standard Terms & Conditions and the Ethical guidelines still apply. In no event shall the Royal Society of Chemistry be held responsible for any errors or omissions in this *Accepted Manuscript* or any consequences arising from the use of any information it contains.

ROYAL SOCIETY OF CHEMISTRY

www.rsc.org/njc

Catalytic performance of in-situ synthesized palladium-polymer nanocomposite

Meenakshi Choudhary, Samarjeet Siwal, Debkumar Nandi and Kaushik Mallick*

Department of Chemistry, University of Johannesburg, P.O. Box: 524, Auckland Park 2006, South Africa.

***Corresponding Author**

E-mail: kaushikm@uj.ac.za

Abstract: Polymer encapsulated metallic palladium nanoparticles have been synthesized by the oxidative polymerization route using a di-amino naphthalene monomer and a palladium based metal salt. The resultant composite material was characterized by means of optical and microscopic techniques, which offered the information about the chemical structure of polymer and also the distribution of the metal particles in the composite material. The palladium nanoparticles were homogeneously dispersed throughout the polymer which produced a uniform metal-polymer composite material. The composite material was successfully used for the hydrogenation reaction of *4*-nitrophenolate ion with the evidence of a proton coupled electron transfer (PCET) reaction mechanism. The palladium-polymer composite material was also used as an iodide sensor for the detection of iodide ion in the presence of other interfering anionic species.

1. Introduction:

The fabrication of functional composite materials with improved properties and performance is an extremely useful step in synthetic materials science. Assembly of the nanocomposites, where the structural order within the material in nanometer scales, is a significant achievement in materials science. Composite architectures of polymer and metal nanoparticles synergistically provide both useful functionality and mechanical integrity. Metal nanoparticles combined with the polymer form a unique composite with interesting physical properties and potential applications. Such composites show various properties which are directly relevant to the dielectrics, energy storage and catalytic applications.[1] Many investigations methods regarding the development of metal-polymer nanocomposite have been reported.[2-4] Recently, 'in-situ polymerization and composite formation' (IPCF) method documented the synthesis of polymer encapsulated metal nanoparticle from their respective monomer and the ionic precursor of metal salt, respectively, in a single step route.[5-10] The method is likely to provide a high degree of synthetic control over both the size of the

nanoparticles and the morphology of the polymer and may be expected to exert a strong influence on the metal-polymer interaction. Polymer stabilized noble metal nanoparticles have attracted much attention recently as a new research direction in various fields of catalysis. The polymer matrices serve both as the support as well as the stabilizer of the nanoparticles thus providing a mechanism to prevent metal agglomeration. Gold-polymer supramolecular composite architecture, Au-Poly (4-amino 3-methylphenol), shows good colorimetric and voltammetric sensor application for the detection of biologically active molecules, where the gold nanoparticles play the role of a catalyst.[11] Again, during the formation of the metal-polymer composite the reduction of the probe molecule follows the proton coupled electron transfer (PCET) reaction mechanism and catalyzed by the metallic counter part of the composite.[12] Polymer encapsulated silver nanoparticles act as catalyst for the electrochemical recognition of hydrogen peroxide.[13] The Pd-polypyrrole nanocomposite material was also used as a catalyst for the electro-catalytic detection of tryptophan[14], an essential amino acid and also precursor for some neurotransmitters.

Palladium nanoparticle based catalysts have recently drawn enormous attention due to their versatile role in organic synthesis.[15, 16] The use of nanosized palladium in catalysis is not only industrially important[17, 18] but also scientifically interesting since they provide a relationship between the catalytic activity and the particle size as well as shape.[19] The well-known application of palladium nanoparticles as a catalyst in synthetic organic chemistry is carbon–carbon bond formation reactions which are commonly used for the synthesis of natural products, pharmaceutical products, fine chemicals and the manufacturing of long chain organic molecules for organo-electronics applications. Among the various carbon–carbon bond formation reactions the Suzuki, Heck and Sonogashira coupling reactions are the most important methods for the synthesis of biaryl products in a single step process. Polyaniline and the derivative of polyaniline stabilized palladium nanoparticles, within the size range of 2-3 nm, show the efficient catalytic activity for Suzuki[20, 21] and Heck[22] coupling reactions under phosphine-free conditions. Dendritic polymer stabilized palladium nanoparticles was found to be a highly effective catalyst for the Sonogashira cross-coupling of aryl halides with terminal alkynes in presence of water as solvent.[23] A single step bottom-up approach has also been documented for the synthesis of Pd-polypyrrole composite with the application of chemoselective transfer hydrogenation of α, β-unsaturated carbonyls.[24] The use of the palladium nanoparticles as an electrocatalyst is also very important in energy related applications. Palladium nanocrystal within the size range of 5-6 nm was used for the oxygen reduction reaction and formic acid oxidation and it was found that oxygen reduction reaction

was strongly depended on the metal structure and the electrolyte used.[25] The control of the nanoscale composition and structure of alloy catalysts plays an important role in heterogeneous catalysis. Palladium nanoparticle based alloy catalysts has been used for the ethanol oxidation reaction in gas phase and in alkaline electrolyte medium.[26] Surface-functionalized carbon nanotube supported palladium alloy nanoparticles was applied as the electrocatalyst for the formic acid electro-oxidation.[27] A facile and one-pot wet chemical approach has been reported for the preparation of palladium based nano-sponge with the great potential for use in fuel cells using methanol or ethanol as fuel and also for the fabrication of electrochemical sensors for the detection of glucose.[28] Palladium nanoparticles decorated single-walled carbon nanotubes showed high electrocatalytic activity as a working electrode for the investigated of hydrazine oxidation by cyclic voltammetry technique.[29] Palladium nanotubes were prepared by using polyol reduction process and displayed high electrocatalytic activity toward the electrooxidation of ethanol.[30]

In this current study, we have synthesized polymer encapsulated palladium nanoparticles within the size range of 2-3 nanometer by applying 'in-situ polymerization and composite formation' method using the precursors 1, 8-diamino naphthalene (as a monomer) and potassium tetrachloro-palladate (K_2PdCl_4, as an oxidizing agent). The synthesized composite material (Pd-*p*DAN) has demonstrated the roll as a catalyst for the electrochemical detection of iodide ion. In this report, we also have showed the application of the composite material for the reduction of *4*-nitrophenolate (*4*-NP) ion in absence of any reducing agent, an example for the proton coupled electron transfer (PCET) reaction mechanism.

2. Experimental:

2.1. Preparation of Pd-*p*DAN composite material: In a typical experiment, 0.158g of 1,8-diaminonaphthalene was dissolved in 10 mL of methanol and a stock solution of K_2PdCl_4 (0.0326 g of K_2PdCl_4 in 10 mL of water) were prepared. In a small glass beaker, 2 mL of K_2PdCl_4 was added to the 5 mL of organic solution under continuous stirring conditions. During the addition, the solution took on a yellow colour, while at the end; a dark brown precipitation was formed at the bottom of the glass beaker. Entire reaction was performed under ambient condition. The material was allowed to settle for 30 min after which the colloidal solution was taken from the bottom of the conical flask and pipetted onto lacey, carbon-coated, copper mesh grids for transmission electron microscopic (TEM) study. The same grid was also used for the scanning electron microscopic (SEM) study. An *in-situ* UV-visible study was also done to get more insight about the polymerization process. The

required amount (10 μL) of the colloidal solution was used to modify the working electrode for the electrochemical studies. The remaining portion of the compound was dried and used for XRD and XPS measurements. For the purpose of control investigation, we have used ammonium persulphate as an oxidizing agent to polymerize 1,8 diaminonaphthalene, with the formation of poly-(1,8 diaminonaphthalene), *p*-DAN, maintaining the molar ratio of 10:1, monomer and oxidizing agent, respectively.

2.2. Material characterization: The UV-vis spectra were measured using a Shimadzu UV-1800 spectrophotometer with a quartz cuvette. Microscopy studies of the nanocomposite were carried out using a JEOL, JEM-2100, Transmission Electron Microscope, equipped with an ultrathin windowed energy dispersive x-ray analysis system (EDX) allowing for the characterization of the microstructure and chemical composition of the material. The SEM studies were performed at 5 kV by using an FEI Quanta 400 instrument. As a precaution to prevent possible charging, the samples were sputter-coated with a thin, uniform layer of Au-Pd. The X-ray diffraction (XRD) patterns were recorded on a Shimadzu XD-3A X-ray diffractometer operating at 20 kV using Cu-Kα radiation (k = 0.1542 nm). The measurements were performed over a diffraction angle range of $2\theta = 10^{o}$ to 80^{o}. X-ray photoelectron spectra (XPS) were collected in a UHV chamber attached to a Physical Electronics 560 ESCA/SAM instrument. Electrochemical measurements were carried out with a, Bio-Logic, SP-200, potentiostat connected to a data controller. A three-electrode system was used in the experiment with a glassy carbon electrode (GCE) as the working electrode. Ag/AgCl electrode (saturated KCl) and a Pt electrode were used as the reference and counter electrodes respectively.

2.3. Hydrogenation study: For this experiment, the probe 4-nitrophenolate (4NP) was made by adding sodium hydroxide to the water solution of 4-nitrophenol with a final concentration of 10^{-6} mol dm^{-3}. The hydrogenation of 4NP was performed in presence of 10 mg of Pd-*p*DAN (2.54 wt% Pd, the value obtained from the quantitative EDS microanalysis method, attached with TEM) and 10 mg of *p*DAN. The progress of the reaction was monitored using a spectrophotometer.

2.4. Electrocatalytic study: Both the polymer, *p*DAN and Pd-*p*DAN composite, were deposited on the working electrode using a 'drop and dry' method. After each run, the electrode was washed and an identical amount of new catalyst was applied as a coating to the electrode for the next study for the electrocatalytic recognition of iodide ion, where potassium iodide (KI) was used as the source of iodide ion.

3. Result and Discussion:

A wide variety of methods have been applied to the preparation of polyaniline or substituted polyaniline-type compounds by the oxidative polymerization of their monomer. In this work, potassium tetrachloro-palladate acted as an oxidizing agent and 1, 8-diamino naphthalene was used as the monomer to form a metal-polymer composite material, respectively. According to the most widely accepted mechanism for the polymerization of the aniline or the substituted aniline involves the release of electron along with a proton.[31, 32-36] The electron was then used to reduce the palladium ion to produce palladium atom. The coalescence of these atoms ultimately forms nanoparticles, which are encapsulated by the polymer.

Figure: 1

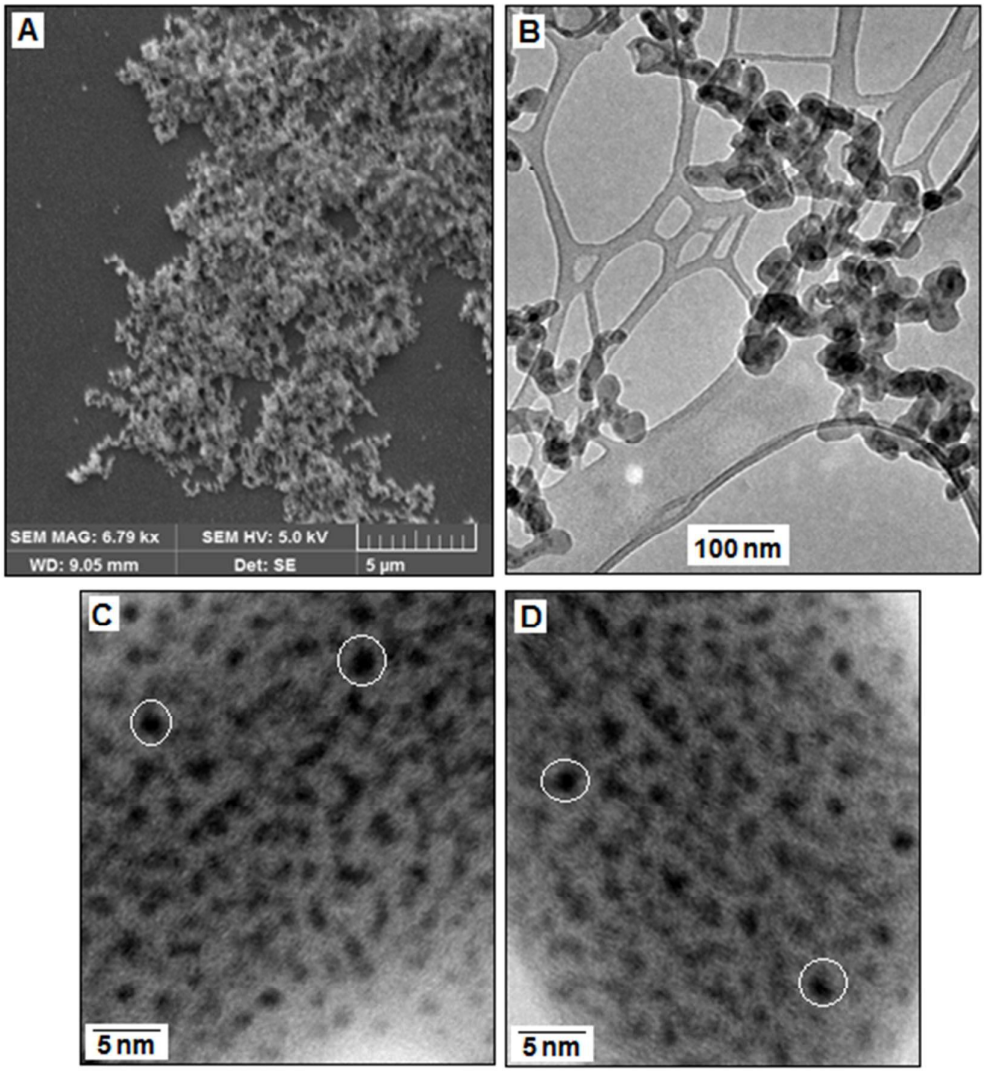

Figure 1: The SEM (A) and the TEM image (B) show the palladium-polymer composite material with a chain like morphology. The higher magnification TEM images (C and D) show the palladium nanoparticles within the size range of 2-3 nm (dark spots) are uniformly distributed (some of them are circled) throughout the composite material.

3.1. Characterization of the resultant compounds:

Figure 1 (A and B) show the SEM and TEM images, respectively, for palladium-polymer composite material with a chain like morphology. The higher magnification TEM images of the material (figure 1, C and D) show the dark spots, within the size range of 2-3 nm, are uniformly distributed (some are circled) throughout the material and the EDS analysis (figure 2A) confirmed that these spots are for the palladium particle.

Figure: 2

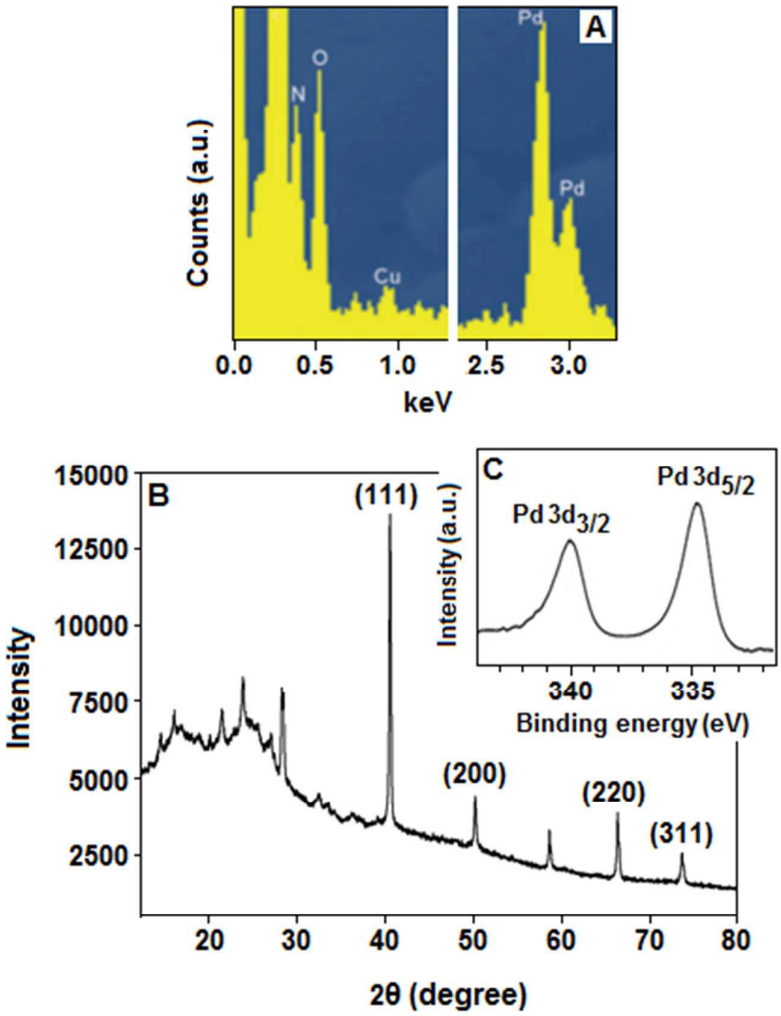

Figure 2: The EDS analysis (A) shows the presence of palladium in the sample. The crystalline nature of the palladium nanoparticles was confirmed by the XRD measurements (B). The strong

Bragg reflection indicates that the Pd-particles are highly oriented, face-selective (111) and crystalline in character. The XPS measurement (C) confirms the metallic character of palladium.

The crystalline nature of the palladium nanoparticles was established by the XRD measurements (Figure 2B). The strong Bragg reflection indicates that the Pd-particles possess a highly oriented, face-selective (111), crystalline character. To identify the chemical state of the palladium particles, XPS measurement was carried out. The Pd 3d region of the XPS spectrum of the Pd-*p*DAN composite is given in figure 2C revealing the presence of both the Pd $3d_{5/2}$ and $3d_{3/2}$ peaks at binding energies of 334.93 and 340.0 eV respectively. These binding energy values are in accordance with those reported for metallic palladium.[37] XPS analysis also confirmed that 2.50 wt% Pd was present on the surface of the polymer support matrix.

Figure: 3

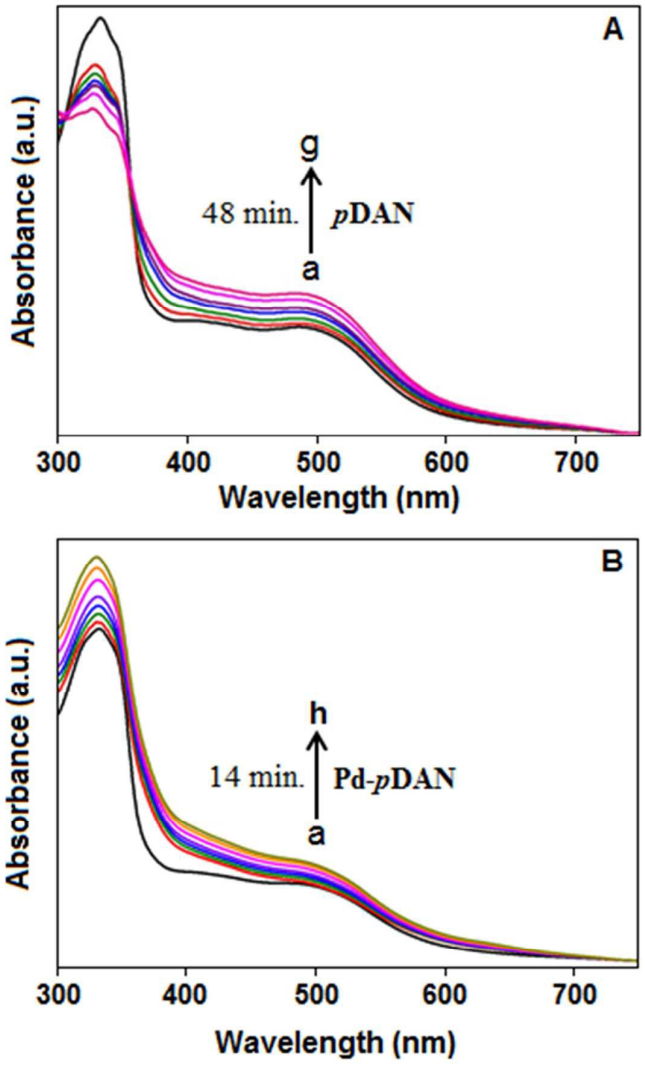

Figure 3: The *in-situ* spectrophotometric studies show the progress of the polymerization reactions of 1, 8-diaminonaphthalene in presence of (A) ammonium persulphate and (B) K_2PdCl_4, respectively. The absorption band with an absorption maxima at 500 nm, correspond to benzenoid to quinoid transition, whereas, the absorption at 325 nm correspond to π-π* transition for both the samples.

The progress of the polymerization reaction was monitored by using UV-visible spectrophotometer (Figure 3). For both the samples a steady increase of the absorption band with an absorption maxima at 500 nm, correspond to benzenoid to quinoid transition, has been observed. The sharp absorption at 325 nm corresponds to π-π* transition has also been observed for both the samples.

3.2. Catalytic property of palladium nanoparticles for PCET reaction:

The polyaniline and its derivatives has become the subject of interest due to its environmental stability, controllable electrical conductivity and interesting redox properties associated with the chain nitrogen. The polymer can exist in a large number of intrinsic oxidation states, which is varied from the fully reduced leucoemeraldine state to the fully oxidized pernigramiline state. The UV-visible spectra shows the gradual transformation from benzenoid (reduced state) to quinoid state (oxidized state) and the transformation can be ceased during the synthesis process if the polymer is taken out from the solvent system and dried. The dry polymer remains in between the states of leucoemeraldine and pernigramiline. To explore the above fact, two sets of experiments have been performed. The dried polymer, Pd-*p*DAN and *p*DAN, were used to study the hydrogenation of 4-nitrophenolate (4-*NP*), a model reaction generally used to check the catalytic property of the material.[38] Polymer immobilized palladium nanoparticles shows good catalytic activity for the reduction of aromatic nitro compounds.[39] In the current experiment, the alkaline aqueous solution of *4-NP* exhibited an absorption peak at 400 nm (Figure 4). Upon the addition of Pd-*p*DAN and *p*DAN to the 4-NP, the intensity of the absorption peak of *4-NP* has been gradually decreased in absence of any reducing agent. The faster rate of quenching of spectra has been observed for Pd-*p*DAN (Figure 4A) as compared with *p*DAN (Figure 4B). The sensible description of the above incident can be explained in the light of proton coupled electron transfer mechanism.[40] When the polymer come in contact with aqueous solution of *4-NP* the oxidation process of the polymer has started again to reach the higher oxidative sate of the polymer, with the release of electron and proton, the mechanism of oxidative polymerization, as mentioned earlier. The released electrons forms the radical cation on the nitrogen of the

nitro group of 4NP (first step of the nitro-group reduction mechanism) followed by the protonation (Scheme 1).

Scheme: 1

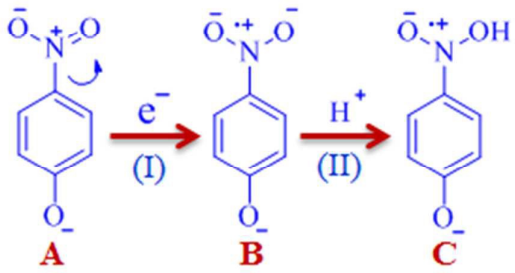

Scheme 1: Reduction of 4NP: A proton coupled electron transfer mechanism.

The above mechanism is considered for the reduction process of 4NP and that causes the quenching of the absorption peak at 400 nm. The quenching of the 4-NP spectra in the presence of Pd-*p*DAN is faster than *p*DAN is due to the presence of palladium nanoparticles, which catalyzed the reduction process of 4-NP with the formation of the 4-aminophenolate (as evidenced by the development of the new peak at 315 nm).[41] Figure 4C shows the plot (C_t/C_0) as a function of time for the reduction of *4-NP* in presence of Pd-*p*DAN and *p*DAN with the rate constant values of 5.7×10^{-3} min^{-1} and 1.61×10^{-2} min^{-1}, respectively.

Figure: 4

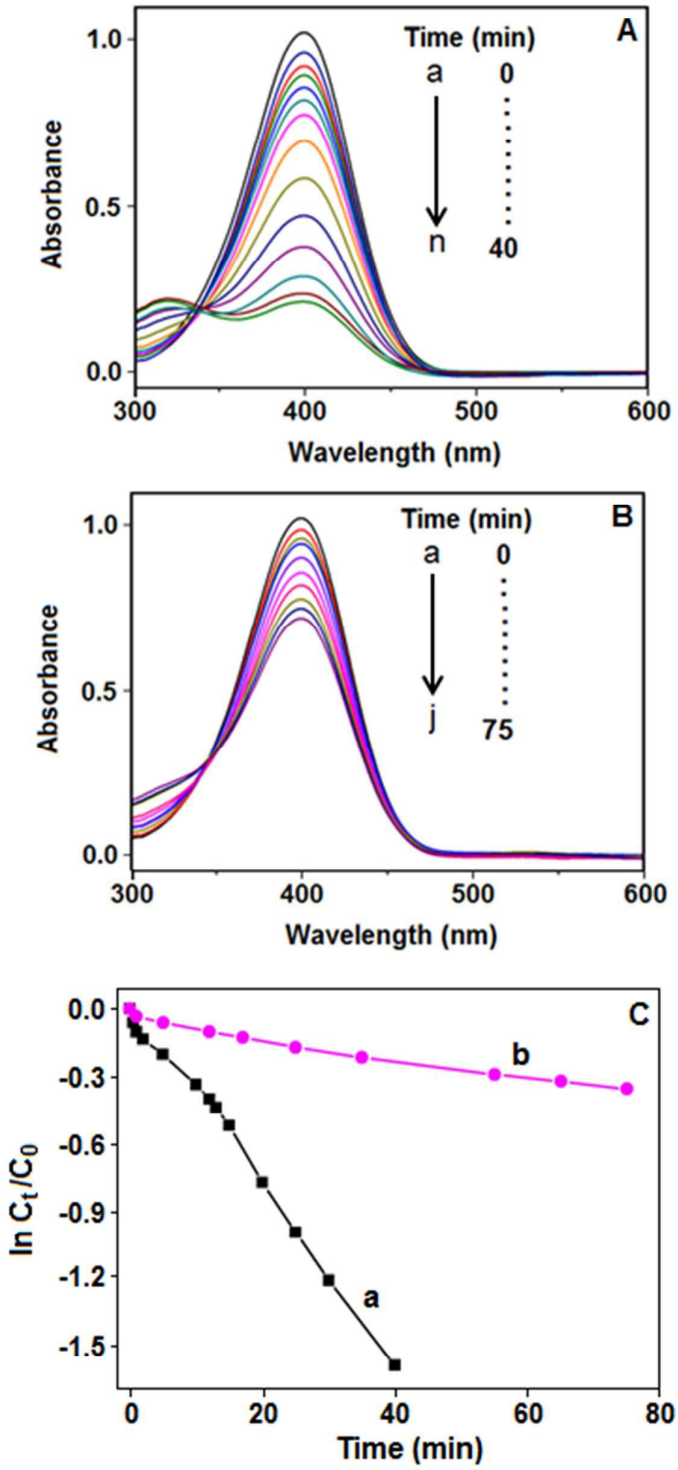

Figure 4: UV-vis spectra show the hydrogenation (reduction) of 4-NP in the presence of (A) Pd-*p*DAN and (B) *p*DAN at different time intervals. (C) Absorption of the 4NP (C_t / C_0, where C_t is the absorption maxima at different time intervals and C_0 is the initial absorption maxima) as a function of time in the presence of Pd-*p*DAN (curve 'a') and *p*DAN (curve 'b')

3.3. Application of Pd-polymer composite for electrochemical iodide ion detection:

The recognition of anions has attracted much attention due to their crucial roles in many biological processes.[42, 43] Among the various biologically important anions, iodide has the enormous importance in physiological system primarily for the synthesis of thyroid hormones.[44] Either deficiency or abundance of iodide can lead to relevant thyroid diseases, such as thyroid enlargement, hypothyroidism and hyperthyroidism. By considering the above facts, early and sensitive detection of iodide is extremely important as the iodine imbalance causing a major health problem throughout the world, particularly for pregnant women and young children.[45] An efficient and early detection is an extremely important step to eradicate the above problems which are caused due to iodide imbalance in our physiological system.

Several attempts have been reported for the sensitive detection of iodide ion. A simple iodide sensing device has been reported based on ultrathin gold films containing optically active holes prepared using a lithography method. The plasmon-active holes were used as an optically active iodide sensor efficiently.[46] Sulphur functionalized gold nanoparticles was reported to develop a colorimetric sensor for the quantitative detection and selective recognition of iodide against other halogen anions.[47] A selective colorimetric sensing system for iodide has been documented by employing an aggregation and re-dispersion strategy of gold nanoparticles with a low detection limit.[48] A colorimetric method has also been described for the sensitive and accurate detection of iodide using citrate-stabilized silver triangular nano-plates.[49] From the literature it is evident that the colorimetric technique was mainly applied for the development of iodide sensor. A potentiometric titration method has been reported for the recognition of iodide ion based on zinc oxide nanotube fabricated on a gold coated glass substrate.[50] Recently, an ultra-fast electrochemical method, based on a silver nanoparticle modified electrode, has been documented for the detection of iodide ion from synthetic urine.[51]

In this current report, we have used Pd-*p*DAN as an electrocatalyst for an efficient detection of iodide ion using an electrochemical method. At first the electrochemical impedance study was performed for the samples, *p*DAN and Pd-*p*DAN, which is a useful technique for probing the features of surface modified electrodes (figure 5). The impedance spectra including a semicircle part at high frequencies, corresponding to the electron transfer limited process and a linear part at lower frequencies, demonstrating the diffusion-limiting step of the electrochemical process. The semicircle diameter equals to the electron transfer resistance at the electrode surface. Figure 5 shows the electrochemical impedance spectroscopy analysis for the Pd-*p*DAN (a) and *p*DAN (b). The straight lines for both the samples are the

characteristic of a diffusion-limiting step of the electrochemical process. For *p*DAN sample the electron transfer resistance was significantly large which indicated the polymer performs as a kinetic barrier for the electron transfer, whereas, in Pd-*p*DAN sample the electron transfer resistance was decreased due to nanometer-sized palladium particles which have participate and promote the electron-transfer process.

Figure: 5

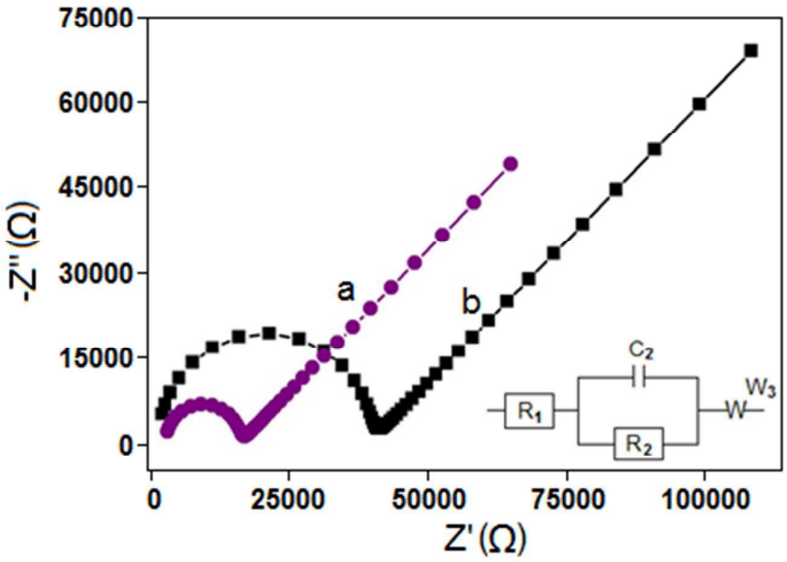

Figure 5: The electrochemical impedance spectroscopy analysis for the (a) Pd-*p*DAN and (b) *p*DAN, modified GCE at pH 7.4 and within the frequency range from 500 kHz to 10 mHz, where, the straight lines for both the samples are the characteristic of a diffusion-limiting step of the electrochemical process. For *p*DAN sample the electron transfer resistance was significantly larger than Pd-*p*DAN sample.

We have compared the affinity and sensitivity of *p*DAN and Pd-*p*DAN for the electrochemical detection of iodide ion using the cyclic voltammetry (CV) technique in milli-Q water, at the scan rate of 50 mV/s^{-1} (Figure 6). The figure 6A represents the cyclic voltammograms for bare GCE in the absence (curve 'a') and presence (curve 'b') of analyte (KI). An enhanced current signal has been observed when KI (50.0 μM) was used as an analyte for bare unmodified electrode. When electrode was modified with *p*DAN, no noticeable enhancement of the anodic current (figure 6B, curve 'a') has been observed, compared to the bare electrode in the absence of analyte (figure 6A, curve 'a'), indicating the stability of the polymer. An enhancement of the anodic peak current for *p*DAN modified electrode in the presence of analyte (50.0 μM of KI) has been noticed (figure 6B, curve 'b'). Figure 6C, the main panel, shows the voltammograms for Pd-*p*DAN modified electrode for

the detection of iodide ion. In the absence of iodide ion, no apparent improvement of the anodic current signal was observed (figure 6C, curve 'a') as compared with the two previous systems (figure 6, A and B, curve 'a'). The Pd-*p*DAN modified GC electrode exhibited enhanced electrocatalytic oxidation in presence of KI (50.0 μM) with the anodic peak current value ~70 μA at the applied potential value 0.575 V (Figure 6C, curve b). These results indicated that palladium-polymer composite exhibited excellent electrocatalytic activity toward the oxidation of KI, and such enhanced activity is due to the introduction of metallic palladium, which reacted with iodide ion and formed PdI_2 species (scheme 2).

Scheme: 2

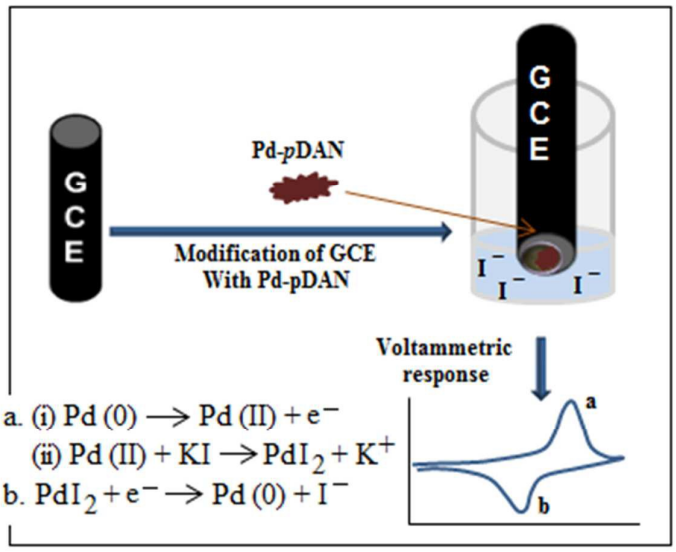

Scheme 2: Schematic diagram of the palladium nanoparticle based iodide sensor.

With increasing concentration of iodide ion the anodic peak height was also increased as evidenced by the cyclic voltammetric study (Figure 6C, curve c-f). The performance of the same catalyst was further studied by differential pulse voltammetry (DPV) technique using various amounts of KI concentration. Figure 6D shows the differential pulse voltammograms with the gradual increase of current intensity (curves: b-h) due to the addition of iodide source (KI) with different concentration (50 to 550 μM). The DP voltammogram (a) represents the zero concentration of iodide ion. It is also important to mention that the minimum concentration of the analyte (KI), which is 50.0 μM, was highly reproducible (100%) for the detection using the Pd-*p*DAN catalyst. Concentration of the KI within the range of 20 – 40 μM was also detectable but reproducibility rate was below 50%, based on ten repeated experiments.

Figure: 6

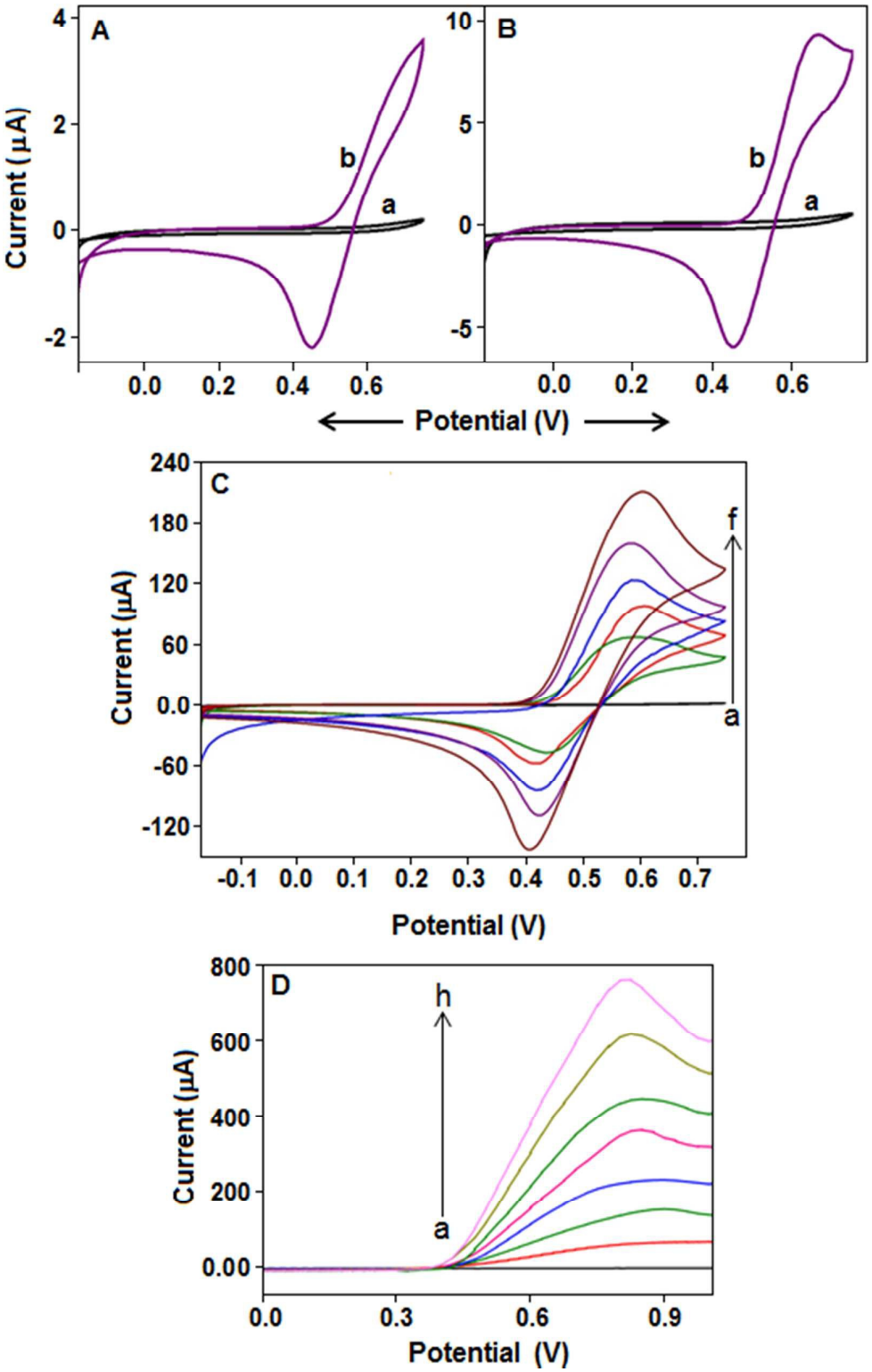

Figure 6: (A) represents the cyclic voltammograms for bare GCE in the absence (curve 'a') and presence (curve 'b') of analyte (KI), (B) represents the cyclic voltammograms for *p*DAN modified GCE in the absence (curve 'a') and presence (curve 'b') of analyte (KI).

(C) shows the voltammograms for Pd-*p*DAN modified electrode for the detection of iodide ion with increasing concentration of KI, curves b–f, 50, 100, 150, 250, 400 μM, respectively, whereas, the voltammogram 'a' is for the absence of KI (in water, at the scan rate of 50 mV/s^{-1}).
(D) represents the differential pulse voltammograms for Pd-*p*DAN modified GCE with the increasing concentration of KI, (b-h), 50, 100, 150, 200, 250, 400, 550 μM, respectively. The voltammogram 'a' is for the absence of KI (in water, at pulse height 25 mV, pulse width 50 ms, step height 25 mV and scan rate 50 mVs^{-1}).

In terms of iodide sensor, stability and selectivity is an important parameter. For an amperometric technique (differential pulsed), a steady increase in current response has been obtained with the addition of iodide, to the electrolyte (milli-Q water). Under the optimized experimental conditions, the presence of some potential interfering species has been investigated. As shown in Figure 7A, in an Pd-*p*DAN modified working electrode system, iodide solution (0.01 M of 50 μL) was injected at first into the N_2-saturated water (10 mL) with an applied potential of 0.6 V, followed by the addition of interferences species (50 μL of 0.01 M $NaHCO_3$, KF, KBr, Na_2CO_3, KCl, Na_2HPO_4, Na_2SO_4, NaAc, $NaNO_3$, I_2, $NaHSO_4$, respectively). The Pd-*p*DAN modified electrode exhibited good passiveness towards electroactive interference species. Further addition of iodide ion in every 50 sec time interval shows a linear increase of current. The regression coefficient and sensitivity value of the sensor was calculated within the time interval from 1100-1750 sec with the values of 0.9967 and 223.29 μA $mM^{-1}.cm^{-2}$, respectively, at 0.6 V (Figure 7B).

Figure: 7

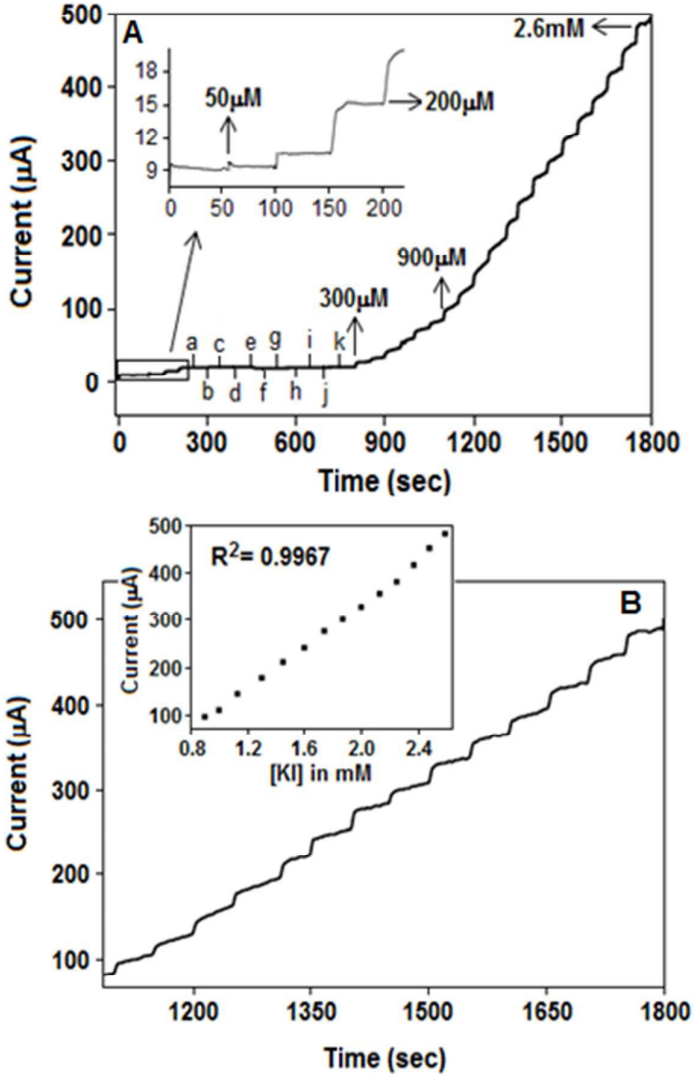

Figure 7: Amperometric response of Pd-*p*DAN modified GCE on successive addition of 50 µL of KI (0.01M) in every 50 sec time interval, under the stirring condition with an applied potential of 0.6 V. The addition of interferences species (50 µL of 0.01 M $NaHCO_3$, KF, KBr, Na_2CO_3, KCl, Na_2HPO_4, Na_2SO_4, NaAc, $NaNO_3$, I_2, $NaHSO_4$,) shows the irresponsive nature towards the amperometric current signal. (B) The regression coefficient and sensitivity value of the sensor within the time interval from 1100-1750 sec are 0.9967 and 223.29 µA mM^{-1}. cm^{-2}, respectively.

4. Conclusion:

We have reported an *in-situ* synthetic route for the preparation of a metal-polymer homogeneous composite material in which 2-3 nm sized palladium particles are highly dispersed in the host polymer matrix, where potassium tetrachloro-palladate and 1, 8-diamino

naphthalene were used as the precursors, respectively. Both the polymer and metal-polymer acted as a reducing agent for the hydrogenation of 4-nitrophenolate (4-*NP*), due to their unsatisfied oxidation state, by following the proton coupled electron transfer reaction mechanism. The composite material, Pd-*p*DAN, shows excellent application towards the recognition of iodide ion in the presence of a wide range of anionic interfering species.

Acknowledgments:

The authors (MC, SS, DKN and KM) acknowledge financial support from the Research Committee and the Faculty of Science of the University of Johannesburg. MC also acknowledges financial support from the National Research Foundation, South Africa. SS and DKN further acknowledge financial support from the Global Excellence and Stature fellowship from the University of Johannesburg.

References:

1. R. Gangopadhyay, A. De, *Chem. Mater.*, 2000, **12**, 608-622.

2. J.J. Watkins, T.J. McCarthy, *Chem. Mater.*, 1995, **7**, 1991-1994.

3. K. Sayo, S. Deki, S. Hayashi, *Eur. Phys. J D*, 1999, **9**, 429-432.

4. J. Lee, V.C. Sundar, J.R. Heine, M.G. Bawendi, K.F. Jensen, *Adv. Mater.*, 2000, **12**, 1102-1105.

5. K. Mallick, M. Witcomb, M. Scurrell, *J. Phys. Condens. Matter,* 2007, **19**, 196225.

6. K. Mallick, M. Witcomb, R. Erasmus, M. Scurrell, *Mater. Sci. Eng. B*, 2007, **140,** 166–171.

7. K. Mallick, M. Witcomb, M. Scurrell, *Eur. Phy. J. E.*, 2007, **20**, 347-353.

8. K. Mallick, M. Witcomb, M. Scurrell, *J. Mater. Sci.*, 2007, **41**, 6189–6192.

9. K. Mallick, M. Witcomb, A. Dinsmore, M. Scurrell, *J. Mater. Sci.*, 2006, **41**, 1733-1737.

10. K. Mallick, M. Witcomb, A. Dinsmore, M. Scurrell, *Langmuir*, 2005, 21, 7964-7967.

11.M. Choudhary, S. Siwal, A. Taher, K. Mallick, *J. Mater. Sci.*, 2015, 50, 6087-6095.

12. M. Choudhary, S. Shukla, R. Islam, M. Witcomb, C. Holzapfel, K. Mallick, *J. Phys. Chem. C*, 2013, **117,** 23009-23016.

13. M. Choudhary, S. Siwal, K. Mallick, *RSC Adv.*, 2015, **5,** 58625-58632.

14. M. Choudhary, R. Islam, M. Witcomb, K. Mallick, *Dalton. Trans.*, 2014, **43**, 6396-6405.

15. E. Negishi, Handbook of Organopalladium Chemistry for Organic Synthesis. Wiley, UK, 2002.

16. J. Tsuji, Palladium Reagents and Catalysts: New Perspectives for the 21st Century. Wiley, UK, 2004.

17. N. Toshima, Y. Wang, *Adv. Mater.*, 1994, **6**, 245-247.

18. A.J. Bard, *Science*, 1980, **207**, 139-144.

19. Y. Mizukoshi, K. Okitsu, Y. Maeda, T.A. Yamamoto, R. Oshima, Y. Nagata, *J. Phys. Chem. B*, 1997, **101**, 7033-7037.

20. R. Islam, M. Witcomb, E. V. D. Lingen, M. Scurrell, W. V. Otterlo, K. Mallick, *J. Organo. Chem.*, 2011, **696**, 2206-2210.

21. R. Islam, M. Witcomb, M. Scurrell, E. V. D. Lingen, W. V. Otterlo, K. Mallick, *Catal. Sci. Technol.*, 2011, **1**, 308–315.

22. R. Islam R, M. Witcomb, M. Scurrell, W.V. Otterlo, K. Mallick, *Catal. Commun.,* 2010, **12**, 116-121.

23. A.L. Isfahani, I.M. Baltork, V. Mirkhani, A.R. Khosropour, M. Moghadam, S. Tangestaninejad, *Eur. J. Org. Chem.,* 2014, **25**, 5603–5609.

24. S. Mahato, R. Islam, C. Acharya, M. Witcomb, K. Mallick, *ChemCatChem*, 2014, **6**, 1419-1426.

25. M. Shao, J. Odell, M. Humbert, T. Yu, Y. Xia, *J. Phys. Chem. C,* 2013, **117**, 4172-4180.

26. J. Yin, S. Shan, M.S. Ng, L. Yang, D. Mott, W. Fang, N. Kang, J. Luo, C.J. Zhong, *Langmuir*, 2013, **29**, 9249-9258.

27. J. Bao, M. Dou, H. Liu, F. Wang, J. Liu, Z. Li, J. Ji, *ACS Appl. Mater. Interfaces*, 2015, **7**, 15223-15229.

28. W. P. Wu, A.P. Periasamy, G.L. Lin, Z.Y. Shih, H.T. Chang, *J. Mater. Chem. A*, 2015, **3**, 9675-9681.

29. D.J. Guo, H.L. Li, *J. Colloid. Interface Sci.,* 2005, **286**, 274-279.

30. Z. Li, H. Lu, Q. Li, X.S. Zhao, P. Guo, *Colloid. Surfaces A*, 2015, **464**, 129-133.

31. S. Bocchini, A. Chiolerio, S. Porro, D. Accardo, N. Garino, K. Bejtka, D. Perrone, C.F. Pirri, *J. Mater. Chem. C*, 2013, **1,** 5101-5109.

32. K. Mallick, M. Witcomb, M. Scurrell, A. Strydom, *Chem. Phys. Lett.*, 2010, **494**, 232-236.

33. K. Mallick, M. Witcomb, R. Erasmus, A. Strydom, *J. Appl. Phys.*, 2009, **106**, 074303.

34. K. Mallick, M. Witcomb, M. Scurrell, A. Strydom, *J. Phys. D: Appl. Phys.,* 2009, **42**, 095409.

35. K. Mallick, M. Witcomb, M. Scurrell, *Eur. Phys. J. E. Soft Matter,* 2006, **20**, 347-353.

36. K. Mallick, M. Witcomb, A. Dinsmore, M. Scurrell, *Macromol. Rapid. Commun.,* 2005, **26**, 232-235.

37. D. Bera, S.C. Kuiry, M. McCutchen, A. Kruize, H. Heinrich, M. Meyyappan, S. Seal, *Chem. Phys. Lett.*, 2004, **386,** 364-368.

38. P. Hervés, M. Pérez-Lorenzo, L.M. Liz-Marzán, J. Dzubiella, Y. Lu, M. Ballauff, *Chem. Soc. Rev.*, 2012, **41**, 5577-5587.

[39] H. Zhao, Y. Wang, R. Wang, *Chem. Commun.,* 2014, **50,** 10871-10874.

40. M. Choudhary, S. Siwal, R. Islam, M. J. Witcomb, K. Mallick, *Chem. Phys. Lett.*, 2014, **608**, 145-151.

41. C. Yuan, Y. Xu, L. Zhong, L. Zhang, C. Yang, B. Jiang, Y. Deng, B. Zeng, N. He, W. Luo, L. Dai, *Nanotechnology,* 2013, **24,** 185602

42. A. F. Danil de Namor, M. Shehab, *J. Phys. Chem. A*, 2004, **108**, 7324-7330.

43. S. Aoki, E. Kimura, *J. Biotechnol.*, 2002, **90**, 129-155.

44. T.K. Malongo, S. Patris, P. Macours, F. Cotton, J. Nsangu, J.M. Kauffmann, *Talanta,* 2008, **76**, 540-547.

45. B. S. Hetzel, *Bull World Health Organ*, 2002, **80**, 410-417.

46. B. Dielacher, R.F. Tiefenauer, J. Junesch, J. Vörös, *Nanotechnology*, 2015, **26**, 025202.

47. L. Chen, W. Lu, X. Wang, L. Chen, *Sensor Actuat. B-Chem,* 2013, **182**, 482-488.

48. G. Zhou, C. Zhao, C. Pan, F. Li, *Anal. Methods*, 2013, **5,** 2188-2192.

49. X. Yang, J. Ling, J. Peng, Q. Cao, Z. Ding, L. Bian, *Anal. Chim. Acta*, 2013, **798**, 74-81.

50. Z. H. Ibupoto, K. Khun, M. Willander, *Sensors*, 2013, **13**, 1984-1997.

51. H.S. Toh, K. Tschulik, C. Batchelor-McAuley, R.G. Compton, *Analyst*, 2014, **139**, 3986-3990.

Table of Contents (TOC)

Multifunctional catalytic performance of the *in-situ* synthesized polymer supported Palladium nanoparticles (Pd NP).

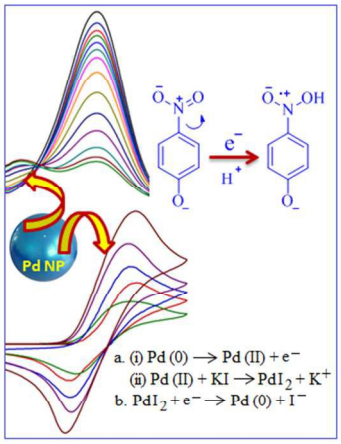

254x190mm (96 x 96 DPI)